Water Air Soil Pollut (2013) 224:1415
DOI 10.1007/s11270-012-1415-y

Particulate and Dissolved Trace Element Concentrations in Three Southern Ecuador Rivers Impacted by Artisanal Gold Mining

Gregory T. Carling · Ximena Diaz · Marlon Ponce · Lester Perez · Luis Nasimba · Eddy Pazmino · Abigail Rudd · Srinivas Merugu · Diego P. Fernandez · Bruce K. Gale · William P. Johnson

Received: 13 September 2012 / Accepted: 5 December 2012 / Published online: 19 January 2013

Abstract Water and sediment samples were collected along river transects at three artisanal gold mining areas in southern Ecuador: Nambija, Portovelo-Zaruma, and Ponce Enriquez. Samples were analyzed for a suite of major and trace elements, including filtered/unfiltered water samples and stream flow measurements to determine dissolved/particulate loads. Results show that the Q. Calixto, Calera, and Siete rivers (corresponding to Nambija, Portovelo-Zaruma, and Ponce Enriquez mining areas, respectively) have substantial trace element contamination due to mining inputs. Dissolved concentrations were elevated at Calera and Siete relative to Q. Calixto, possibly reflecting the input of soluble cyano-metal complexes in mining zones where cyanidation is used in ore processing. A negative correlation was found between MeHg:THg ratios and pH, indicating an inverse relationship of mercury methylation with cyanidation (since cyanidation increases water pH). This was the first comprehensive study to

Electronic supplementary material The online version of this article (doi:10.1007/s11270-012-1415-y) contains supplementary material, which is available to authorized users.

G. T. Carling · E. Pazmino · A. Rudd · S. Merugu · D. P. Fernandez · W. P. Johnson (✉)
Department of Geology & Geophysics, University of Utah, Salt Lake City, UT, USA
e-mail: william.johnson@utah.edu

X. Diaz
Department of Extractive Metallurgy, Escuela Politécnica Nacional, Quito, Ecuador

M. Ponce · L. Nasimba
Instituto Nacional de Investigación Geológico Minero Metalúrgico, INIGEMM, Quito, Ecuador

L. Perez
Instituto Nacional de Meteorología e Hidrología, INAMHI, Quito, Ecuador

B. K. Gale
Department of Mechanical Engineering, University of Utah, Salt Lake City, UT, USA

Present Address:
G. T. Carling
Department of Geological Sciences, Brigham Young University, Provo, UT, USA

examine an extensive suite of trace elements in both water and sediment at the three main gold mining areas of southern Ecuador, including dissolved and particulate loads, and the first study to report MeHg concentrations in the mercury-contaminated rivers.

Keywords Cyanidation · Methyl mercury · Trace metals · Particulate loads · Dissolved loads · Ecuador

1 Introduction

Artisanal gold mining is a substantial source of mercury contamination in developing countries worldwide (Appleton et al. 1999; Cordy et al. 2011; Taylor et al. 2005). In southern Ecuador, subterranean artisanal gold mining is mainly focused in three areas: Nambija, Portovelo-Zaruma, and Ponce Enriquez (Fig. 1). Mining history, including methods for gold extraction, and geology of each area are described briefly below, and in more detail in Appleton et al. (2001). Limited regulations and lack of enforcement has led to extensive pollution in rivers draining the mining areas (Cardenas and Escarate 2005; Lovitz 2006). This paper describes concentrations and loads of mercury and other trace elements in the primary drainages of Nambija, Portovelo-Zaruma, and Ponce Enriquez mining areas: Q. Calixto, Calera, and Siete, respectively.

The Nambija area is a chaotic gold-rush typical town that has been extensively worked by small-scale miners. Most of the mining and processing occurs in the town of Nambija, which is drained by Rio Q. Calixto (Fig. 1). Gold occurs primarily in vugs and veins within and close to skarn bodies developed on volcano-sedimentary rocks (Fontbote et al. 2004); it is recovered by gravimetric concentration and amalgamation with mercury. The residues are deposited in the ground or are discarded to nearby streams. Q. Calixto, the most severely impacted stream in the area, ultimately flows to the Amazon Basin (Fig. 1).

The Portovelo-Zaruma mining district has around 110 small-scale active metallurgical plants (Guimaraes et al. 2011). Rio Calera drains most of the Portovelo-Zaruma mining district, and the processing plants are situated adjacent to the river (Fig. 1). Gold occurs in multi-phase mineralization including base-metal-rich mesothermal and base-metal-poor epithermal assemblages; it is recovered by a combination of amalgamation with mercury and leaching with cyanide. Mining waste is stored in lined and unlined tailings ponds or discharged directly to nearby streams. The Calera and Amarillo rivers are two of the main tributaries of the Puyango River which flows south to Peru then west to the Pacific Ocean (Fig. 1).

The Ponce Enriquez mining district has around ten small-scale active metallurgical plants (J. Ruilova, personal communication). A majority of the processing plants in the Ponce Enriquez area are located along Rio Siete (Fig. 1). Gold occurs in arsenopyrite–pyrrhotite–chalcopyrite hydrothermal veins; it is recovered by a combination of amalgamation with mercury and leaching with cyanide. Mining waste is stored in lined and unlined tailings ponds or discharged directly to nearby streams, which drain to the Rio Siete. Rio Siete follows a short reach from the mountains to the coastal plain, where there are extensive banana plantations and shrimp farms, to the Pacific Ocean (Fig. 1).

Most previous studies on contamination in southern Ecuador mining areas have focused on the Puyango River basin (Portovelo-Zaruma area), including Betancourt et al. (2005), who measured Hg, Mn, and Pb in river water and sediment to determine pathways of human exposure to these elements; Tarras-Wahlberg et al. (2001), who examined Cd, Cu, Hg, Pb, and Zn concentrations in river water, sediment, and biota to determine bioavailability of these elements; and Tarras-Wahlberg and Lane (2003), who measured suspended sediment loads and associated metal contamination. Ramirez-Raquelme et al. (2003) provided Hg measurements in stream sediment and soils at the Nambija area. Other studies, including Velasquez-Lopez et al. (2010, 2011) and Tarras-Wahlberg (2002) focused on artisanal mining processes in southern Ecuador with the goal of developing methods to decrease mercury contamination.

Appleton et al. (2001) and Tarras-Wahlberg et al. (2000) are the only previously published studies that have compared water and sediment chemistry between the three main mining areas in southern Ecuador (Nambija, Portovelo-Zaruma, and Ponce Enriquez). Our work builds upon these previous studies by providing (1) additional data for As, Cd, Cu, Hg, Pb, Ni, and Zn to compare with data collected in the mid- to late-1990s; (2) data for a wider range of elements, including Cr, Co, Ni, V, Se, and Sb, that were not analyzed as part of previous investigations; (3) particulate and dissolved trace element concentrations in streams at all three mining areas; and (4) stream flow measurements, which were used to calculate loads.

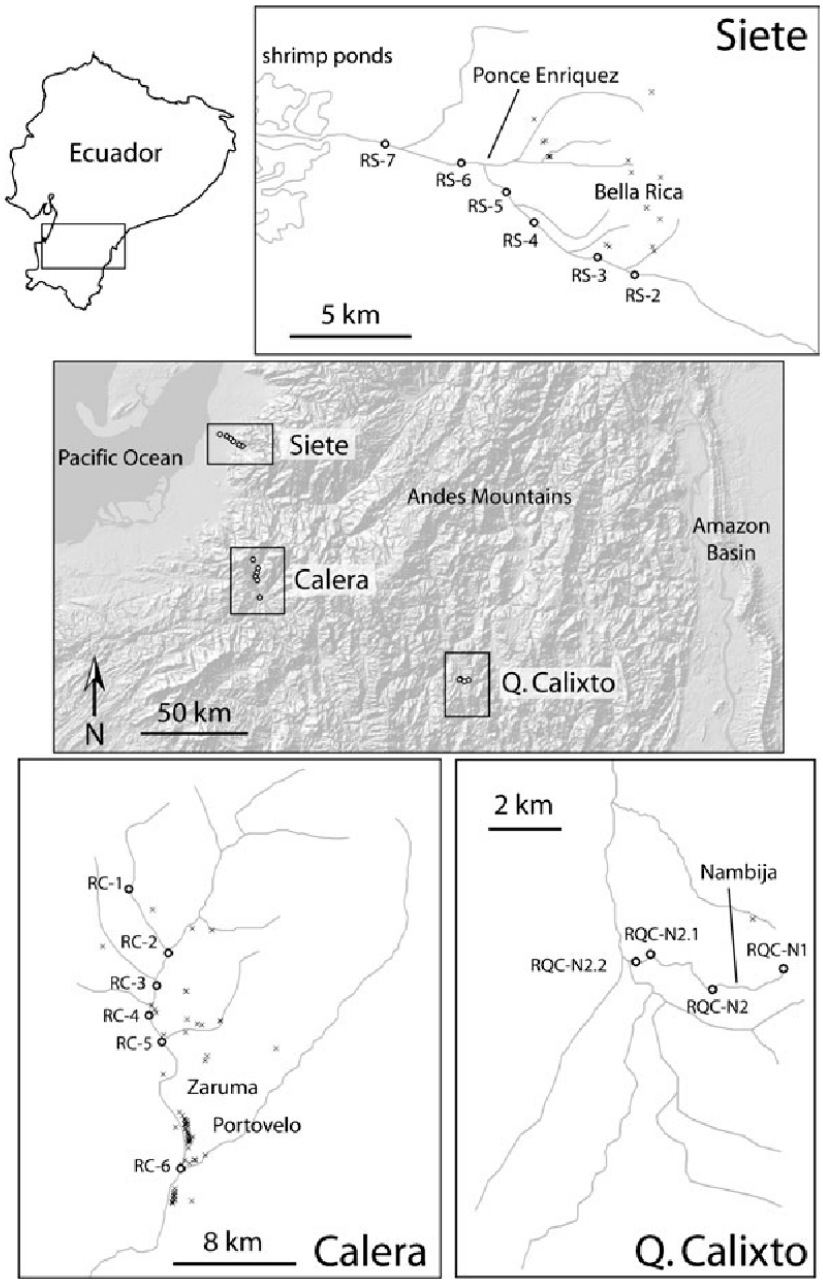

Fig. 1 Map of southern Ecuador mining zones showing location of sample sites (circles), ore processing plants ("x"), major towns, and other important features along each transect

Furthermore, despite well-known occurrence of Hg contamination in mining-affected streams in southern Ecuador, to our knowledge, no measurements of methyl Hg (MeHg) concentrations in stream water are reported in the literature. MeHg, the most toxic and bioaccumulative form of Hg, is produced in aquatic systems by sulfate- and iron-reducing bacteria in the presence of organic matter (e.g., Benoit et al. 2003; Kerin et al. 2006; Lambertsson and Nilsson 2006). MeHg is potentially a serious problem in the organic carbon-rich streams of southern Ecuador (Appleton et al. 2001). Notably, although MeHg concentrations are not reported, Guimaraes et al. (2011) measured methylation potential in sediment from the Puyango River basin (Portovelo-Zaruma). They found low methylation rates downstream of mining operations, which they attributed to the negative effect of cyanide on methylating bacteria.

This investigation has the following objectives with respect to the Nambija, Portovelo-Zaruma, and Ponce-Enriquez mining areas: (1) contrast trace element concentrations (including a wide range of trace elements) in river water and sediment along mining-impacted transects; (2) compare dissolved and particulate trace

element concentrations in relation to ore mineralogy and milling processes in each area; (3) provide a "snapshot" of trace element loads; and (4) characterize MeHg concentrations in the mercury-contaminated rivers.

2 Methods

2.1 Sample Collection

Co-located water and sediment samples were collected along river transects at Nambija (Rio Q. Calixto), Portovelo-Zaruma (Rio Calera), and Ponce Enriquez (Rio Siete) to characterize stream chemistry upstream, within, and below gold mining-impacted zones during low flow conditions of the dry season (Fig. 1). These streams were selected for sampling because they drain the most heavily impacted zones within each mining area. Along Q. Calixto, a majority of the mining and milling activity occurs within the town of Nambija; thus, one sample (RQC-N1) was collected upstream of Nambija to assess background conditions, and the remaining three samples (RQC-N2, RQC-N2.1, and RQC-N2.2) were collected downstream of Nambija. At Calera and Siete, mining and milling activities are distributed along the stream reach; mills are marked with an "x" in Fig. 1. Samples were collected upstream of the mining zones on Calera and Siete (RC-1 and RS-2, respectively), and the remaining samples (RC-2 through RC-6 and RS-3 through RS-7, respectively) were collected within the mining zone along the reach of either stream below the confluence of significant tributaries.

Samples were collected at Q. Calixto, Calera, and Siete on 24–25, 27, and 30 June 2010, respectively. Since water quality in artisanal mining areas shows significant temporal variability due to sporadic releases of contaminants from processing activities, the concentrations represent "snapshot" measurements. Furthermore, seasonal changes in flow were not accounted for since measurements were made only during a short period. Our objective was to provide a snapshot of dissolved and particulate trace element concentrations and loads at Q. Calixto, Calera, and Siete during the dry season when concentrations are expected to be highest; the relationships between sites may be different during the rainy season due to increased flow.

2.2 Water Sample Collection and Analyses

"Clean hands, dirty hands" protocols (USEPA Method 1669) were used during all steps of the sampling process, and new vinyl gloves were used for each set of water samples. All bottles, filters, and other sampling equipment were pre-cleaned prior to sampling (via 10 % HCl leach and/or triple rinse with Milli-Q water). Water samples at Q. Calixto transect were filtered using 0.45 μm PES syringe filters and 50 mL plastic syringes; samples at Calera and Siete transects were filtered using 0.45 μm PES cartridge filters and PTFE tubing. Samples were collected from the middle of the stream below the surface, upstream of where the operators were standing, to obtain a well-mixed representative sample. Trace metal grade acids were used for sample preservation, and samples were stored on ice or refrigerated until analysis.

Filtered (<0.45 μm) and unfiltered water samples were collected for total Hg (THg), MeHg, trace elements (Ag, Al, As, Ba, Be, Cd, Co, Cr, Cu, Fe, Li, Mn, Mo, Ni, Pb, Sb, Se, Sr, Ti, Tl, U, V, and Zn), and major cations (Ca, K, Mg, and Na). Filtered samples were collected for dissolved organic carbon (DOC) and major anions (Cl^-, NO_3^-, and SO_4^{2-}). DOC samples were filtered using glass fiber filters. Alkalinity was measured on unfiltered samples.

Field blanks were collected for each measured parameter at Q. Calixto and Calera (total of two field blanks for each constituent) to test for contamination during the sampling process, including filtering (syringe versus cartridge filters), storage, and handling of samples. Field blanks showed that the background for most constituents was below the detection limit (Supporting Information). For constituents with measureable background, the concentrations were negligible compared to concentrations measured in samples.

THg and MeHg water samples were collected in 250-mL FLPE bottles, acidified in the field to 1 % *v*/*v* HCl, and analyzed within 6 months using a Brooks Rand Model III cold vapor atomic fluorescence spectrometer (CVAFS). THg and MeHg concentrations were determined according to USEPA Methods 1631 and 1630, respectively. THg samples were prepared using in-bottle BrCl oxidation, and MeHg samples were distilled prior to analysis. At a minimum, matrix spike recoveries and replicates were analyzed for every ten samples. For the sample run to be accepted, matrix spike recoveries had to fall within 75–125 % of

the original sample run, and replicate analyses had to fall within ±10 %. Method blanks were analyzed at the beginning of each run in order to calculate a daily detection limit (DL). Typical values of DL were 0.2 and 0.01 ng/L for THg and MeHg, respectively. USGS standard reference sample Hg-47 was analyzed four times during the THg sample runs to check the method, with results within ±7 % of the most probable value (Supporting Information). No standard reference sample exists for MeHg; however, our analyses of three samples provided by the 2011 Brooks Rand Labs Interlaboratory Comparison Study were within ±10 % of the most probable values (Supporting Information).

Samples for trace elements and major cations were collected in 30-mL (filtered) and 60-mL (unfiltered) LDPE bottles, acidified to 2.4 % *v*/*v* HNO_3, and analyzed within 6 months using an Agilent 7500ce quadrupole inductively coupled plasma mass spectrometer (ICP-MS) with a collision cell. USGS standard reference sample T-201 was analyzed six times during the sample run as a continuing calibration verification and to check the method. The reference solution showed that element concentrations were within ±0–15 % of accepted values for all elements except Se (−38 %) (Supporting Information). The inaccuracy in Se measurements may be due to Se instability in the T-201 solution since it contained no Se stabilizer and had been stored nearly 1 year prior to analysis. We feel confident that this difference was not the result of Ar and Cl interferences on the ICP-MS measurement, since Se and As were measured using kinetic discrimination (H_2 in the collision cell), a method which has been shown to effectively eliminate spectral interferences (e.g., Beisner et al. 2009).

Major anion samples were analyzed within 2 weeks by ion chromatography (IC), and alkalinity samples were analyzed on the day of collection by titration. DOC samples were collected in amber glass bottles and analyzed within 1 month using a Shimadzu TOC-5000A. Field parameters, including water temperature (T_w), conductivity, pH, and dissolved oxygen (DO), were measured at each sampling site using a YSI Quatro multiparameter field probe. The probe was calibrated for conductivity, pH, and DO at the beginning of each sampling day.

Major ion charge balances were within an acceptable range of ±5 % for 6 out of 16 samples, and 2 samples were within ±10 % (Supporting Information). The remaining eight samples had charge balance errors between −11 % and −25 %, indicating an underestimation of cations or overestimation of anions. A majority of the samples with large error were visibly turbid samples; thus, HCO_3 (measured as total alkalinity on unfiltered samples) may have been overestimated. Regardless of the cause of error, the differences in ion concentrations between sites along each transect (factor of 3 or more) were much larger than charge balance errors.

2.3 Geochemical Modeling

Aqueous speciation and saturation indices (SI) were estimated with PHREEQC using the Minteq.v4 thermodynamic database (Parkhurst and Appelo 1999). Positive SI values, calculated as log (IAP/K_{sp}), indicate oversaturation and thermodynamic potential for mineral precipitation. PHREEQC uses ion-association and Debye Hückel expressions to account for the nonideality of aqueous solutions. T_w, pH, and dissolved concentrations of major ions and trace elements measured at each site were used in the simulations.

2.4 Particulate Versus Dissolved

The fraction of trace element mass associated with ≥0.45 μm suspended solids, or particulate fraction, was calculated as the difference between unfiltered and filtered concentrations. The fraction passing through the filter was considered dissolved. Although the mass of a trace element that passes through a 0.45-μm filter is not necessarily dissolved, as the trace element may be associated with colloidal phases <0.45 μm, we hereby use the term "dissolved" for simplicity of discussion. Filtered concentrations <DL were set as one-half DL to calculate particulate fraction and for all further analysis. In a limited number of cases where filtered concentrations were greater than unfiltered concentrations, the difference was typically within analytical error (+0–15 %), and the element was considered entirely dissolved.

In order to determine the distribution of trace elements among the range of particle sizes in the >0.45-μm fraction, a total of 11 water samples (5 from Calera and 6 from Siete) were size-fractionated via steric mode asymmetric flow field flow fractionation (AsFlFFF) using an AF2000 (Postnova Analytics). Size fractions ranging from 0.45 to 20 μm were collected and analyzed for THg and trace elements. The operating conditions used for this method were detector flow=2.5 mL/min, slot flow=2 mL/min, injection flow=0.3 mL/min, focus time=7 min, and transition time=2 min. The cross flow

rate was constant (1.5 mL/min) from 0 min to 6 min of elution, and then decreased linearly to zero from 6 to 9 min of elution, followed by 2 min of rinsing. The channel thickness was 315 μm. Discrete fractions were collected from 0–2, 2–3, 3–4, 4–5, 5–7, 7–10, to 10–13 min. This process was repeated six times to achieve sufficient volume of each fraction for analysis by ICP-MS and CVAFS. An example fractogram showing elution time of calibration standards is shown in the Supporting Information. Water samples for AsFlFFF were shipped overnight from Ecuador to the University of Utah, and fractionation was completed within 3 days of sample collection.

2.5 Loads

Stream flow was measured at all sampling sites except RC-1, RS-6, and RS-7 using an OTT Hydromet propeller (model C-31). Velocity measurements were taken in a cross-sectional area, every 0.5 to 1 m in width, and between 2 and 5 measurements in depth. The average stream velocity and the flow discharge were calculated using the number of revolutions of the propeller, the cross-sectional area of the river, the number of measurements at each point (width and depth), and the characteristic equation of the propeller. Particulate and dissolved trace element loads were calculated from concentration and flow data. Loads were not calculated for RC-1, RS-6, or RS-7 due to lack of flow measurements.

2.6 Sediment Sample Collection and Analysis

Bed sediment was collected immediately downstream of water sample sites, sieved to isolate the <70-μm size fraction, and dried at room temperature. Final dry sample size was ~100 g. Sediment was digested by Aqua Regia and analyzed by ICP-MS for a suite of trace and major elements at AcmeLabs (Vancouver, BC, Canada).

3 Results

3.1 Trace Element Concentrations in Mining Impacted Rivers

Trace element concentrations increased dramatically upon entering the mining zones, with concentrations increasing by orders of magnitude from upstream to downstream (Figs. 2 and 3). Of all the measurements made on sediment and water samples, this paper focuses primarily on 15 elements: As, Cd, Co, Cr, Cu, Hg, Mn, Ni, Pb, Sb, Se, Ti, U, V, and Zn. For Hg, results are shown for both THg and MeHg.

The most dramatic increase in trace element concentrations occurred at the upstream end of Q. Calixto and Siete and at the downstream end of Calera. In all three transects, this reflects the location of the highest density of processing plants in the mining zone (compare Fig. 1 with Figs. 2 and 3). Calera and Siete showed higher dissolved concentrations than Q. Calixto for most elements (Figs. 2 and 3, Supporting Information).

Different trace elements were predominant among the three transects, defining a unique signature for each mining sector. Co, Cr, Hg (both THg and MeHg), Mn, Ni, Ti, U, and V concentrations were highest at Q. Calixto, whereas As, Cd, Pb, and Se concentrations were highest at Calera (Figs. 2 and 3). Q. Calixto and Calera showed similarly high values of Cu and Zn, while Calera and Siete showed similarly high values of Sb (Figs. 2 and 3). Although data are not shown, Calera was the only transect with substantial concentrations of Ag (Supporting Information).

USEPA guidelines for drinking water and/or protection of freshwater aquatic life were exceeded by dissolved concentrations at all three transects (Figs. 2 and 3). Drinking water guidelines for Mn were exceeded by a wide margin (factor of >5) at Q. Calixto and Siete, and were barely exceeded at Calera. Drinking water guidelines for As were exceeded by a factor of 6 at Calera and by nearly a factor of 2 at Siete. Guidelines for Sb were exceeded by a factor of 3 at Calera and by a factor of 10 at Siete. In contrast, As and Sb guidelines were not exceeded at Q. Calixto. Cu drinking water guidelines, as well as Ag, Cd, and Pb criteria for protection of aquatic life, were exceeded only at Calera. Notably, although particulate concentrations of some elements (including THg, Al, and Fe) exceeded guidelines by orders of magnitude, the dissolved fraction of these elements did not exceed guidelines.

In contrast to the trace elements, major ion chemistry and field parameters were similar among the three transects (Supporting Information). All three transects had low major ion concentrations (dominated by Ca, SO_4, and HCO_3), low conductivity, and low DOC concentrations. Field measurements indicated well-mixed conditions (>75 % DO saturation) and slightly alkaline conditions (7.4<pH<8.1) at all transects. The only exception was the furthest downstream site at Calera (RC-

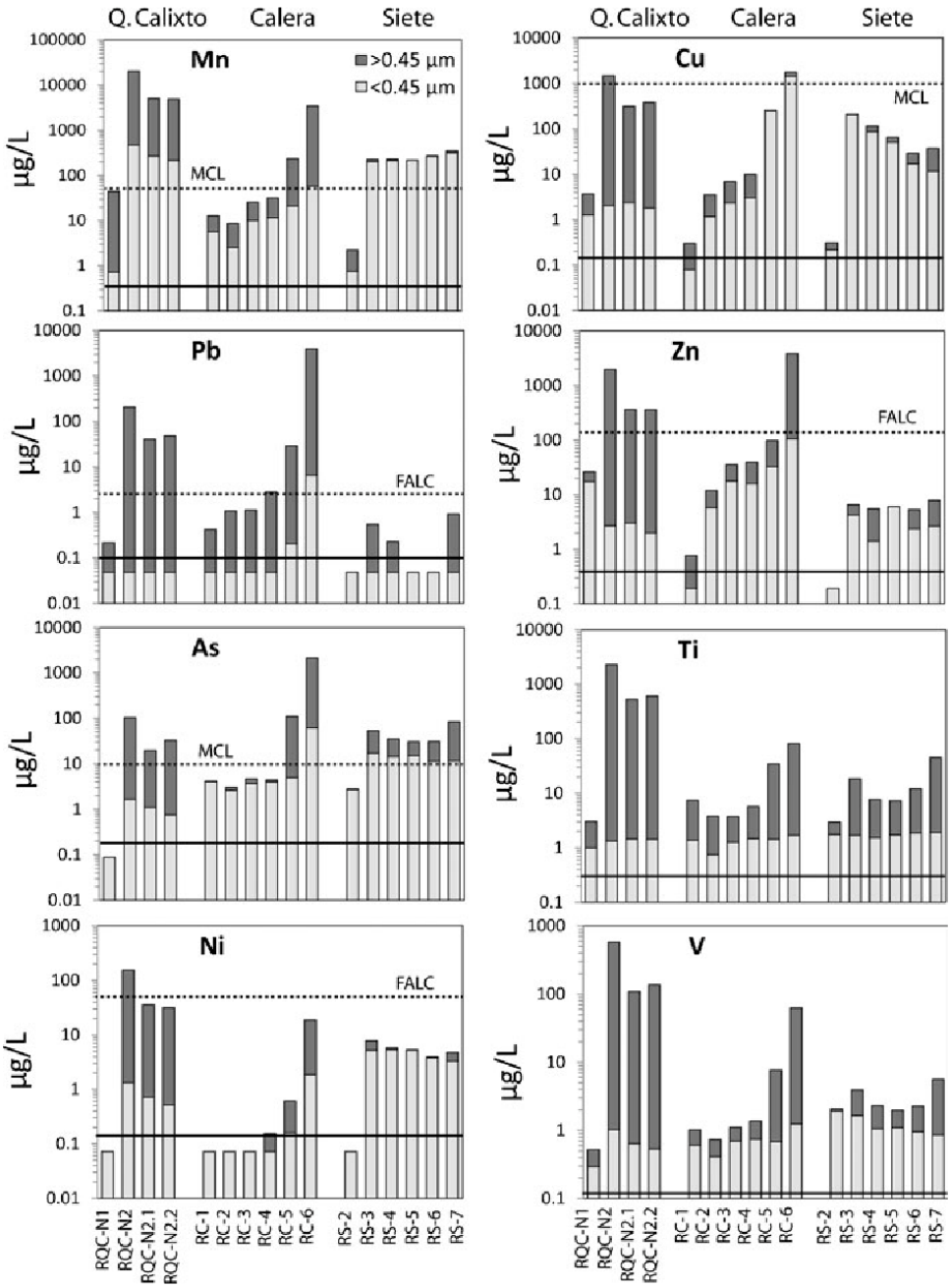

Fig. 2 Dissolved (<0.45 µm) and particulate (>0.45 µm) trace element concentrations at each sample site along the Q. Calixto, Calera, and Siete transects. *Dashed lines* show USEPA Maximum Contaminant Level (MCL) or Freshwater Aquatic Life Criteria (FALC) values. *Solid lines* show the detection limit (DL) for each element; values <DL are reported as one-half DL

6), where pH was more strongly alkaline (pH=9.0) due to the large number of cyanidation plants near the site (Fig. 1). During the cyanidation process, lime ($Ca(OH)_2$) is added to the slurry to obtain a pH above 10 (Velasquez-Lopez et al. 2011).

3.2 Trace Element Concentrations in Bed Sediment

Trace element concentrations in sediment at the farthest downstream site of each transect (Fig. 4) showed that Calera had the highest concentrations of As, Cu, Pb, Zn, Co, Cd, Sb, and Se among the three transects, while Q. Calixto had the highest Mn and U concentrations, and Siete had the highest Ti, V, Cr, and Ni concentrations. Data for all measured elements are provided in the Supporting Information.

Environment Canada sediment guidelines for protection of aquatic life were exceeded at all three transects (Fig. 4). Sediment guidelines for Hg were exceeded at all transects, reflecting extensive use of mercury amalgamation in the mining process. Sediment guidelines for As and Cu were barely exceeded at Q. Calixto, but

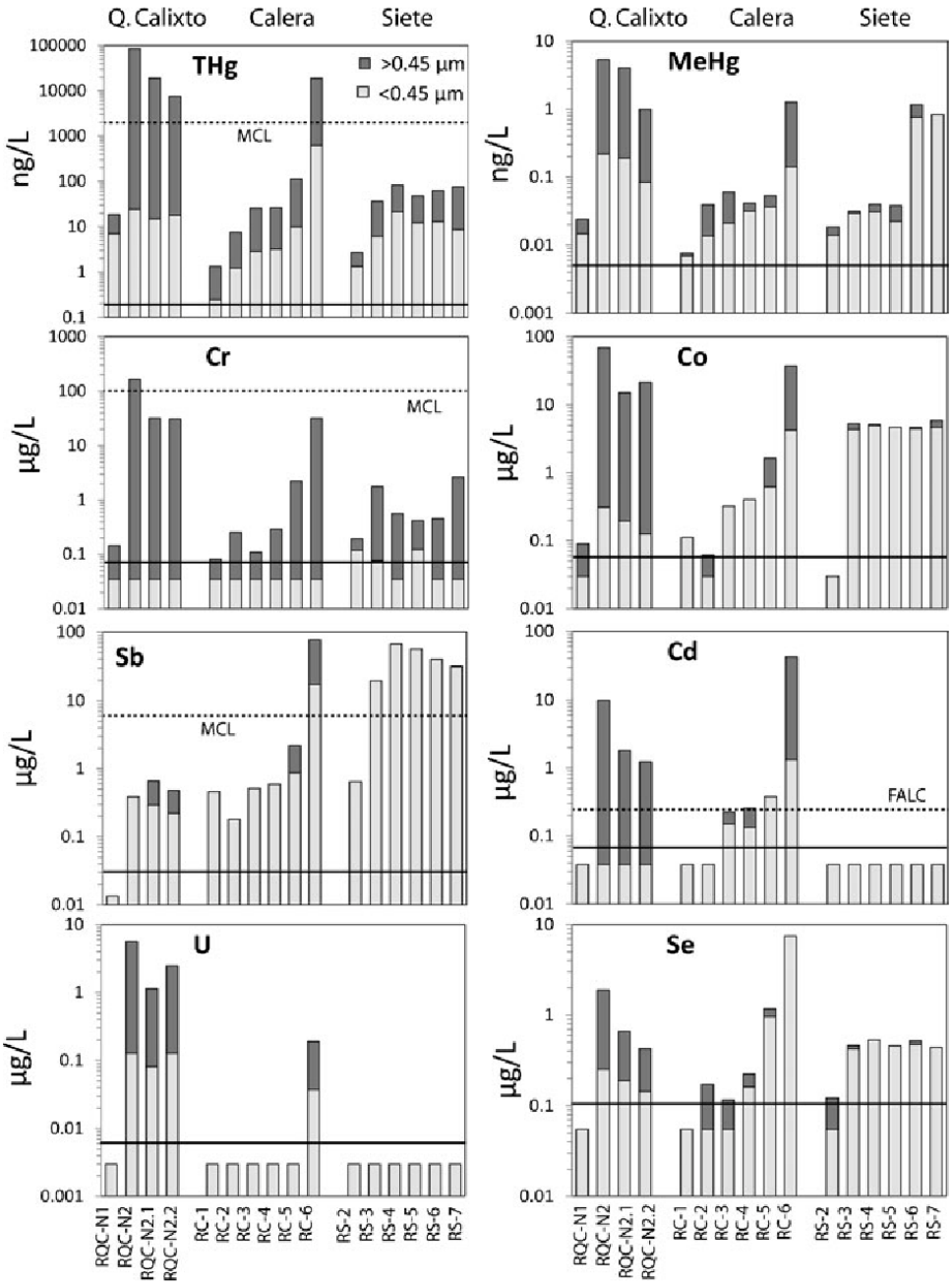

Fig. 3 Dissolved (<0.45 μm) and particulate (>0.45 μm) trace element concentrations at each sample site along the Q. Calixto, Calera, and Siete transects. *Dashed lines* show USEPA Maximum Contaminant Level (MCL) or Freshwater Aquatic Life Criteria (FALC) values. *Solid lines* show the detection limit (DL) for each element; values <DL are reported as one-half DL

exceeded by a wide margin (factors of >10) at Calera and Siete. Additionally, guidelines for Cd, Pb, and Zn were exceeded only at Calera (by a factor of >10), and Cr guidelines were exceeded only at Siete.

3.3 Spatial Distribution of Trace Element Loads

Trace element concentrations were converted to loads using stream flow measurements, as described in Section 2.5. Among the three transects, the largest trace element loads were found at the downstream site at Calera (RC-6). This was true for both dissolved and particulate loads, as shown in Figs. 5 and 6, respectively. Pie charts were used in Figs. 5 and 6 in order to simplify comparison of loads across the Q. Calixto, Calera, and Siete rivers. In the pie charts, elements were grouped as follows: (1) high concentration trace metals Cu, Mn, Pb, Ti, and Zn; (2) intermediate concentration trace metals Cd, Cr, Co, Ni, and THg; and (3) anion-forming trace elements As, Sb, Se, U, and V. While these groupings are somewhat arbitrary, of the variety of groupings that were explored, these were

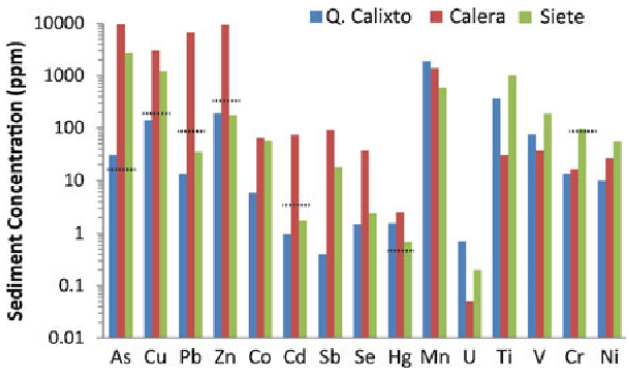

Fig. 4 Sediment trace element concentrations (parts per million) at downstream sites of Q. Calixto (RQC-N2.2), Calera (RC-6), and Siete (RS-7). *Dashed lines* indicate Environment Canada probable effect level

determined to provide the best possible contrast of all elements between transects.

At Calera and Siete, loads increased from upstream to downstream. At Q. Calixto, dissolved loads were relatively constant from upstream to downstream below the mining zone, whereas particulate loads decreased substantially (Figs. 5 and 6, respectively). Loads were highest at Calera because of high concentrations and highest stream flow among the three rivers (maximum 4.97 m^3/s). Q. Calixto and Siete had only moderate trace element loads, in contrast to high concentrations along these transects, because of their relatively low flow (maximum 0.33 and 1.57 m^3/s, respectively) (Supporting Information). At Q. Calixto and Calera, particulate loads were orders of magnitude greater than dissolved loads (compare scales on Figs. 5 and 6), indicating that the majority of trace element transport in these rivers is associated with suspended sediment, whereas at Siete, dissolved loads were greater than particulate loads.

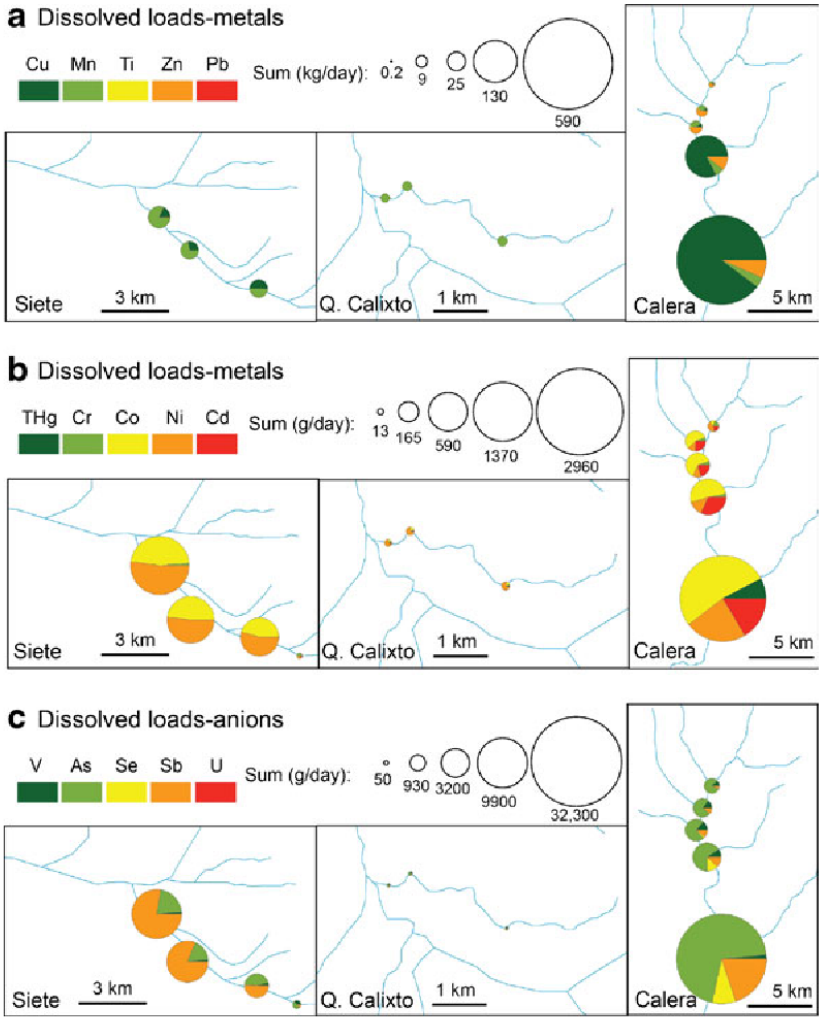

Fig. 5 Dissolved loads of (**a**) Cu, Mn, Ti, Zn, and Pb; (**b**) THg, Cr, Co, Ni, and Cd; and (**c**) V, As, Se, Sb, and U at Siete, Q. Calixto, and Calera transects. Units are kilograms per day for **a**, and grams per day for **b** and **c**. The pie charts show relative contributions of each element at each sample site. The pie area is proportional to the sum of loads of the five elements represented in the pie

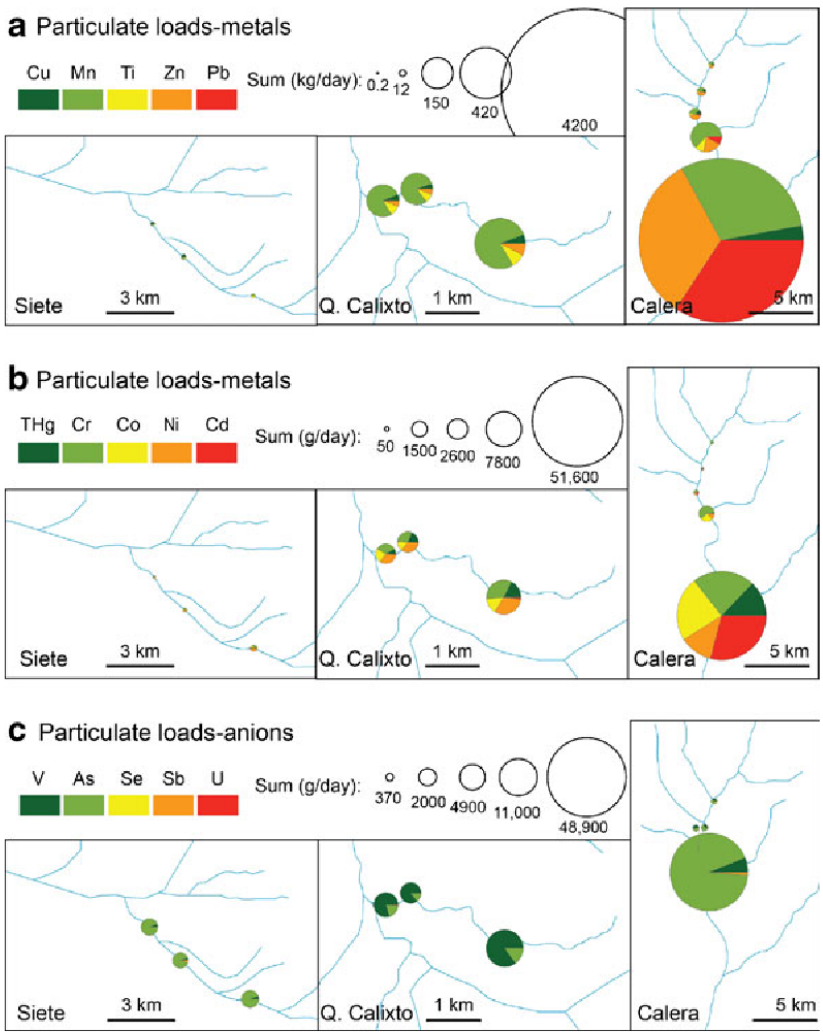

Fig. 6 Particulate loads of (**a**) Cu, Mn, Ti, Zn, and Pb; (**b**) THg, Cr, Co, Ni, and Cd; and (**c**) V, As, Se, Sb, and U at Siete, Q. Calixto, and Calera transects. Units are kilograms per day for **a**, and grams per day for **b** and **c**. The pie charts show relative contributions of each element at each sample site. The pie area is proportional to the sum of loads of the five elements represented in the pie. In **c**, data for the downstream-most site at Calera (RC-6) are not shown because the load was too large (>800,000 mg/day) to plot at the same scale as loads from the other sites

4 Discussion

4.1 Geochemical Relationship to Ore and Processing

The trace element contamination at each mining district is expected to be a function of local geology and the predominant mode of mining used in the area. The gold-bearing ore at Nambija presents high-grade gold accompanied in most deposits by very low Fe, Cu, Zn, and Pb sulfide content (Fontbote et al. 2004). These characteristics may help explain the lower metal concentrations found in Q. Calixto sediment relative to Calera and Siete (Fig. 4). The ore at Portovelo-Zaruma contains elevated Ag, Cu, Pb, Zn, As, Cd, and Bi in epi/mesothermal veins (Williams et al. 2000). Accordingly, Calera had elevated Ag concentrations in sediment (Supporting Information), and it was the only transect with high Ag concentration in water (Supporting Information). Furthermore, Cu, Pb, Zn, and As were the dominant trace elements in Calera water and sediment, and Calera had the highest Cd concentrations of the three mining areas (Figs. 3 and 4). Although Bi was not measured in water samples, Calera had the highest Bi concentrations in sediment (Supporting Information). The ore at Ponce Enriquez contains elevated As, Sb, Cu, Pb, and Ag in mesothermal veins (Williams et al. 2000). Accordingly, As, Sb, and Cu (along with Mn) were the predominant trace elements in Siete water (Figs. 2 and 3), and fairly high concentrations of Pb and Ag were measured in sediment (Supporting Information).

The three transects were also distinguished by different modes of mining used to recover gold. All three mining zones use mercury amalgamation to recover gold, thus all three areas show elevated mercury contamination. However, in addition to mercury amalgamation, cyanidation is used extensively at Ponce Enriquez and Portovelo-Zaruma, but not at Nambija.

Cyanide tends to form stable dissolved complexes in the water column (Tarras-Wahlberg et al. 2000). In particular, Pb, Cd, and Hg are known to form cyano complexes that may become soluble in the water column during tailings disposal (Kyle et al. 2011). The use of cyanidation perhaps explains the higher dissolved concentrations at Siete and Calera (Ponce Enriquez and Portovelo-Zaruma) relative to Q. Calixto (Nambija; Figs. 2 and 3). The fraction of trace element mass found in the dissolved form was also much higher in Siete and Calera relative to Q. Calixto, especially for THg, Ti, V, Cu, and Zn (Table 1).

4.2 Remediation of Mining Contamination

Settling of particulate elements, sorption of dissolved elements to bed sediment, and mineral precipitation are three potential mechanisms for removing trace elements from the mining-impacted streams. Due to the elevated particulate element loads at Q. Calixto and Calera (Fig. 6), the majority of trace element mass could potentially be removed from these rivers via settling ponds. AsFlFFF results indicated that trace elements were in fact associated with particles much larger than 0.45 μm, as shown in Fig. 7 for five representative elements from Calera site RC-6. Association with particles in the larger size ranges would lead to rapid settling of trace elements. Notably, particulate loads at Q. Calixto decreased downstream from the town of Nambija, likely due to settling of suspended solids (Fig. 6).

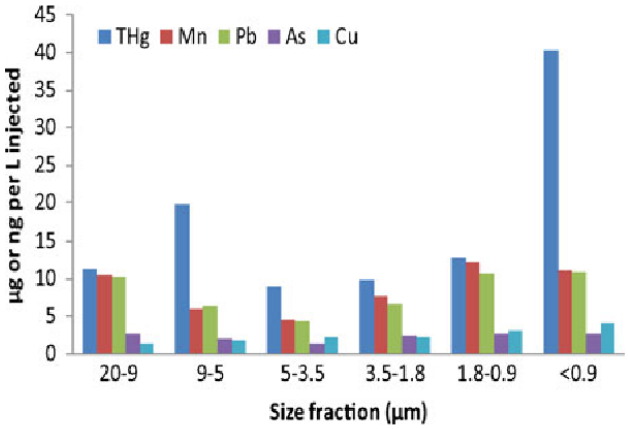

Fig. 7 The distribution of representative trace elements among the range of particle sizes between 0.45 and 20 μm, as determined by asymmetric flow field flow fractionation. Data are from Calera site RC-6. Concentrations were normalized to injection volume; masses are nanograms for Hg and micrograms for all other elements

Sorption to bed sediment could remove large amounts of dissolved trace elements from the aqueous phase. Sorption is a function of temperature, pH, aqueous speciation, and surface characteristics, with cation sorption favored by increasing temperature and pH, and anion sorption favored by decreasing temperature and pH (Dzombak and Morel 1990; Fuller and Davis 1989; Machesky 1990). This leads to some

Table 1 Trace element mass found in the dissolved fraction (percent) at Q. Calixto, Calera, and Siete sample sites

		THg	Ti	V	Cu	Zn
Q. Calixto	RQC-N1	37.8	32.8	56.4	34.5	65.5
	RQC-N2	0.0	0.1	0.2	0.1	0.1
	RQC-N2.1	0.1	0.3	0.6	0.8	0.8
	RQC-N2.2	0.2	0.2	0.4	0.5	0.6
Calera	RC-1	18.5	18.6	59.8	26.7	24.9
	RC-2	16.4	19.8	55.7	32.8	48.2
	RC-3	11.0	34.4	62.9	33.9	49.8
	RC-4	12.2	25.8	54.1	30.3	40.4
	RC-5	8.7	4.2	8.9	100	33.1
	RC-6	3.3	2.1	2.0	81.3	2.8
Siete	RS-2	49.4	59.2	92.4	69.7	100
	RS-3	16.7	9.2	41.9	100	64.3
	RS-4	25.8	19.9	45.8	74.4	25.6
	RS-5	25.4	23.6	55.5	77.5	100
	RS-6	20.7	15.3	41.9	59.0	44.7
	RS-7	11.6	4.2	15.4	31.8	33.7

difficulties for removing both cations and anions. For example, removal of dissolved metals (abundant at Siete and Calera; Fig. 5) would require increasing the solution pH. An increase in pH could in turn mobilize sorbed anion-forming trace elements. Between sites RC-5 and RC-6 at Calera, where pH increased from 8 to 9, dissolved anion loads increased proportionally more than dissolved metal loads (factor 10 increase for anions compared to factor of 5 increase for metals; Fig. 5). Notably, Se was predicted as a selenate oxyanion (+VI oxidation state) at all sites except RC-6, where it was predicted as a selenite oxyanion (+IV oxidation state). Selenite species are less likely to sorb onto bed sediment than selenite species (Hyun et al. 2006), potentially leading to higher concentrations in the aqueous phase. Indeed, dissolved Se concentrations were elevated at the downstream sites of Calera (Fig. 3).

PHREEQC-calculated saturation indices showed that minerals containing Cu, Sb, Fe, and Mn had thermodynamic potential for mineral precipitation at Calera and/or Siete. Cu-containing minerals, such as azurite, malachite, and cuprite, were oversaturated at Calera and Siete due to elevated Cu concentrations in the rivers, and SbO_2 was oversaturated at Siete due to elevated Sb concentrations. Furthermore, a number of minerals containing Fe and Mn, including goethite (FeOOH) and rhodochrosite ($MnCO_3$), were oversaturated at the downstream site at Calera (RC-6). Of course, kinetic limitations may inhibit formation of mineral precipitates.

4.3 Mercury Methylation

Total MeHg concentrations were highest at Q. Calixto, whereas dissolved MeHg concentrations were highest at Siete (Fig. 3). Although concentrations provide useful information, MeHg:THg ratios are often used in order to understand in situ methylation processes (Mitchell et al. 2008). Dissolved MeHg:THg ratios ranged over several orders of magnitude (from 0.02 % to nearly 10 %) among the three transects, reflecting very different rates of in situ MeHg production (Fig. 8). Typical MeHg:THg background ratios in aqueous systems are around 1 % (Gray and Hines 2009). Thus, high ratios (approaching 10 %) at the downstream end of Siete (RS-6 and RS-7) indicate that substantial methylation is occurring at these sites.

Although a majority of trace elements, field parameters, and major ions were similar at downstream and upstream sites of Siete, RS-6 and RS-7 did show a lower pH than the other sites (Figs. 2 and 3; Supporting Information). Furthermore, the water was darker and more organic-rich at RS-6 and RS-7 relative to all other sites, reflecting wastewater inputs and runoff from nearby agricultural and municipal sources. The stream also had a lower velocity at RS-6 and RS-7 relative to all other sites. Further work should investigate methylation potential along Rio Siete to determine causes of elevated MeHg:THg ratios.

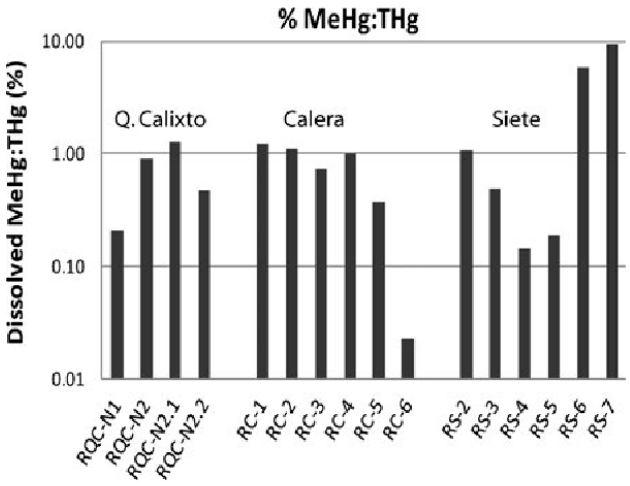

Fig. 8 Dissolved MeHg:THg ratios in filtered water samples from all sites

Notably, MeHg:THg ratios decreased along the Calera and Siete transects from RC-1 through RC-6 and from RS-2 through RS-5, respectively (Fig. 8). Cyanidation is used in the mining process at both Calera and Siete, which is likely at least partly responsible for low MeHg:THg ratios at sites near processing plants (compare Fig. 1). A negative correlation between cyanide and mercury methylation potential was shown by Guimaraes et al. (2011), who found low methylation potential in the Puyango River watershed sediments (including Calera) due to elevated cyanide concentrations. MeHg is produced several kilometers downstream of cyanidation plants, possibly reflecting rapid degradation of cyanide away from processing plants.

Although cyanide concentrations were not measured as part of this investigation, the potential negative correlation between cyanide and mercury methylation is demonstrated by using pH as a proxy for cyanide, since the cyanidation process increases water pH (Velasquez-Lopez et al. 2011). The highest MeHg:THg ratios were found at RS-6 and RS-7, which had the lowest pH, whereas the lowest MeHg:THg ratios were found at RC-6, which had the highest pH (Fig. 9).

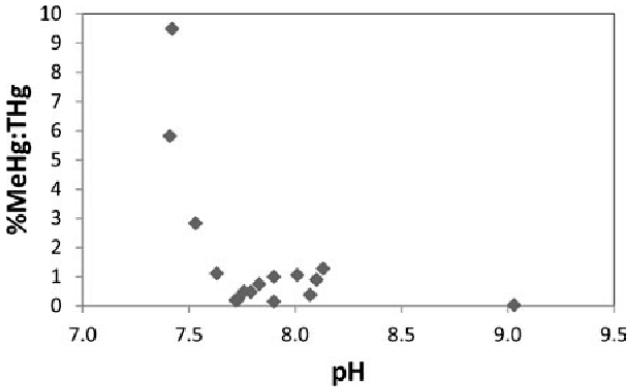

Fig. 9 Relationship between dissolved MeHg:THg ratios and pH for all sample sites

High dissolved MeHg:THg ratios at Siete (Fig. 8) demonstrate the potential for production of toxic MeHg in mining-impacted streams. At Siete, MeHg could pose a threat to the commercial banana plantations and shrimp farms downstream of mining activity. Furthermore, loading of MeHg to the mangroves and bays could negatively impact fisheries along the coastline. Further work is needed to measure Hg concentrations in shrimp, bananas, and fish adjacent to mining impacted areas, and in people who consume those products, as proposed by Appleton et al. (2001).

Although MeHg:THg ratios were low at Calera and Q. Calixto (Fig. 8), these transects showed elevated loads of inorganic mercury; thus, areas downstream could be negatively impacted by production of MeHg. For example, inorganic mercury from Q. Calixto could be methylated in the organic carbon-rich rivers of the Amazon Basin (e.g., Dominique et al. 2007). Tarras-Wahlberg et al. (2001) speculated that MeHg is likely produced in the Puyango River (downstream of Calera) based on elevated levels of Hg measured in biota.

4.4 Relationship of Water Chemistry to Sediment Chemistry

Elements with the highest concentrations in river sediment also showed the highest particle-associated concentrations in the overlying water. Cu and Mn were the dominant trace metals in both suspended particles and sediment at all three transects (Fig. 2). Additionally, Calera had high concentrations of Pb and Zn in both phases, whereas Siete and Q. Calixto had high concentrations of Ti. Arsenic was the dominant anion-forming element in both phases at Siete and Calera (Figs. 2 and 4). Notably, both As and V were the dominant anion-forming elements at Q. Calixto, with V showing higher concentrations in both phases. At Siete, dissolved Sb concentrations were a factor of 10 higher than dissolved As concentrations, even though As concentrations were much higher in sediment. This finding agrees with Hiller et al. (2012), who showed that under oxidizing conditions, Sb was released from solids more efficiently than As. U concentrations were highest at Q. Calixto in both the water and sediment (Figs. 3 and 4).

Table 2 Filtered trace element concentrations (micrograms per Liter) in streams draining the Ponce Enriquez, Portovelo-Zaruma, and Nambija mining zones as reported in this study and others

Drinking water guidelines[a]		Ponce Enriquez			Portovelo-Zaruma			Nambija		
		a	b	c	a	b	c	a	b	c
As	10	17.1	470	264	61.7	nd	6.8	1.7	nd	2.9
Cd	5	<0.076	9	0.05	1.32	41	0.7	<0.076	<4	<0.005
Cu	1,000	208	7,277	11.1	1,434	437	23.2	2.4	3.5	1.3
Hg	2	0.021	0.9	–	0.617	0.1	–	0.025	0.1	–
Ni	–	5.4	165	–	1.9	35	–	1.3	<10	–
Pb	15	<0.096	nd	2.0	6.5	nd	2.5	<0.096	<40	0.157
Zn	5,000	6.1	821	–	105	3,354	–	3.0	<5	–

[a] USEPA drinking water maximum contaminant level

a: this study; maximum concentrations

b: Appleton et al. (2001); maximum concentrations

c: Tarras-Wahlberg et al. (2000); representative concentrations during dry season

Table 3 Trace element concentrations (parts per million) in bed sediment of streams draining the Ponce Enriquez, Portovelo-Zaruma, and Nambija mining zones as reported in this study and others

Probable effect level[a]		Ponce Enriquez			Portovelo-Zaruma			Nambija		
		a	b	c	a	b	c	a	b	c
As	17	3,968	46,049	7,700	1,313	7,493	403	34	34	1,860
Cd	3.5	2.2	24	6.05	72.9	104	19.6	1.1	3.0	47.8
Cu	197	1,425	9,134	2,500	2,993	8,750	1,680	219	409	5,360
Hg	0.49	1.4	13	2.0	2.5	3.0	0.1	2.0	34	2.2
Pb	91	35.4	666	70.6	6,646	10,524	1,310	13.3	42	4,470
Zn	315	175	924	–	9,304	9,792	–	211	231	–

[a] Environment Canada sediment quality for protection of aquatic life

a: this study; maximum concentrations

b: Appleton et al. (2001); maximum concentrations

c: Tarras-Wahlberg et al. (2000); representative concentrations during dry season

4.5 Comparison to Previous Work

Tables 2 and 3 show the maximum concentrations in filtered water and bed sediment, respectively, as reported in this study, Appleton et al. (2001), and Tarras-Wahlberg et al. (2000). All three studies show that the Nambija mining area has the lowest trace element concentrations in water (Table 2). Of the three studies, Appleton et al. (2001) reported the highest concentrations (for all elements) at Ponce Enriquez (Rio Siete). At Portovelo-Zaruma (Rio Calera), both this study and Appleton et al. (2001) reported higher concentrations than Tarras-Wahlberg et al. (2000), who collected samples from a different tributary (Rio Amarillo). This reflects lesser degree of contamination in Amarillo relative to Calera due to the fewer number of cyanidation plants (Fig. 1). All three studies report As values at Ponce Enriquez that exceed USEPA drinking water quality guidelines (Table 2). Furthermore, the three studies show that dissolved Hg, Pb, and Zn do not exceed water quality guidelines at any of the three mining areas. Of the three studies, Appleton et al. (2001) was the only to report Cd concentrations that exceed guidelines (at both Ponce Enriquez and Portovelo-Zaruma), whereas this study is the only to report Cu values exceeding guidelines (at Portovelo-Zaruma only).

Sediment quality results from this study are similar to those reported in Tarras-Wahlberg et al. (2000) for Ponce Enriquez and Portovelo-Zaruma mining areas, and similar to Appleton et al. (2001) for Nambija (Table 3). Appleton et al. (2001) reported the highest concentrations in sediment at both Ponce Enriquez and Portovelo-Zaruma, whereas Tarras-Wahlberg et al. (2000) reported the highest concentrations for Nambija. All three studies reported As and Cu concentrations that exceeded Environment Canada sediment quality guidelines at all three mining zones. Hg exceeded the guidelines in most cases. Furthermore, the studies agree that Cd, Pb, and Zn exceed guidelines at Portovelo-Zaruma, but the results for these elements are mixed for the other mining zones.

5 Conclusions

Artisanal gold mining at the Nambija, Portovelo-Zaruma, and Ponce Enriquez areas of southern Ecuador has led to downstream trace element contamination exceeding environmental guidelines in the Q. Calixto, Calera, and Siete rivers, respectively. Cyanidation appears to have an effect on the amount of dissolved trace elements discharged to the rivers, with elevated dissolved concentrations at Siete and Calera (where cyanidation is used to extract gold) relative to Q. Calixto (where only mercury amalgamation is used). The fraction of trace element mass in the dissolved and particulate forms has important implications for downstream transport and remediation. Dissolved trace elements remained in solution downstream of processing plants at Siete, while particulate elements settled out of the

water column downstream of Nambija. Whereas the particle-associated fraction of trace elements can potentially be removed from the water column using settling ponds, removal of the dissolved fraction would require much more complex chemical processes such as sorption or mineral precipitation.

High methyl mercury to total mercury ratios at the downstream sites of Siete indicate that in situ mercury methylation is occurring in the organic carbon-rich, slow moving reaches of the river. MeHg:THg ratios were lowest near cyanidation plants, where pH was highest, indicating a negative correlation between methylation and cyanidation. Further work is needed to understand the controls on methylation in these mining areas.

Acknowledgments This work was conducted under a project-scoping award (0964836) from the US National Science Foundation Office of International Science and Education. Any opinions, findings, and conclusions or recommendations expressed in this material are those of the authors and do not necessarily reflect the views of the National Science Foundation. We wish to thank Dr. Diósgrafo Chamba, former Executive Director of the Ecuadorian Agency of Regulation and Control for Mining (ARCOM), and the Ecuadorian National Institute of Research in Geology, Mining and Metallurgy (INIGEMM) for providing personnel for field work as well as vehicles and drivers for transportation to field sites. We also thank Met. Carlos Naranjo, Executive Director of the Ecuadorian National Institute of Meteorology and Hydrology (INAMHI) for providing personnel and equipment for flow measurements in the rivers. We thank Roberto Garcia for providing GIS maps of the study areas. We are grateful to the drivers and other field assistants for making this work possible and feasible, and to mine operators who allowed access to their property for sampling.

References

Appleton, J. D., Williams, T. M., Breward, N., Apostol, A., Miguel, J., & Miranda, C. (1999). Mercury contamination associated with artisanal gold mining on the island of Mindanao, the Philippines. *Science of the Total Environment, 228*(2–3), 95–109.

Appleton, J. D., Williams, T. M., Orbea, H., & Carrasco, M. (2001). Fluvial contamination associated with artisanal gold mining in the Ponce Enriquez, Portovelo-Zaruma and Nambija areas, Ecuador. *Water, Air, and Soil Pollution, 131* (1–4), 19–39.

Beisner, K., Naftz, D. L., Johnson, W. P., & Diaz, X. (2009). Selenium and trace element mobility affected by periodic displacement of stratification in the Great Salt Lake, Utah. *Science of the Total Environment, 407*(19), 5263–5273.

Benoit, J. M., Gilmour, C. C., Heyes, A., Mason, R. P., & Miller, C. L. (2003). Geochemical and biological controls over methylmercury production and degradation in aquatic ecosystems. In Y. Cai & O. C. Braids (Eds.), *Biogeochemistry of environmentally important trace elements* (Acs Symposium Series, Vol. 835, pp. 262–297). Washington: American Chemical Society.

Betancourt, O., Narvaez, A., & Roulet, M. (2005). Small-scale gold mining in the Puyango River Basin, southern Ecuador: a study of environmental impacts and human exposures. *EcoHealth, 2*(4), 323–332.

Cardenas, C., & Escarate, S. (2005). *Con organizacion y responsabilidad construiremos nuestro futuro. Sistematizacion de la experiencia de explotacion minera de Bella Rica y Guananche Tres de Mayo*. Quito: Centro Ecuatoriano de Derecho Ambiental (CEDA).

Cordy, P., Veiga, M. M., Salih, I., Al-Saadi, S., Console, S., Garcia, O., et al. (2011). Mercury contamination from artisanal gold mining in Antioquia, Colombia: the world's highest per capita mercury pollution. *Science of the Total Environment, 410–411*, 154–160.

Dominique, Y., Muresan, B., Duran, R., Richard, S., & Boudou, A. (2007). Simulation of the chemical fate and bioavailability of liquid elemental mercury drops from gold mining in Amazonian freshwater systems. *Environmental Science and Technology, 41*(21), 7322–7329.

Dzombak, D. A., & Morel, F. M. M. (1990). *Surface complexation modeling: hydrous ferric oxide*. New York: Wiley.

Fontbote, L., Vallance, J., Markowski, A., & Chiaradia, M. (2004). Oxidized gold skarns in the Nambija District, Ecuador. *Society of Economic Geologists, Special Publication, 11*, 341–357.

Fuller, C. C., & Davis, J. A. (1989). Influence of coupling of sorption and photosynthetic processes on trace element cycles in natural waters. *Nature, 340*(6228), 52–54.

Gray, J. E., & Hines, M. E. (2009). Biogeochemical mercury methylation influenced by reservoir eutrophication, Salmon Falls Creek Reservoir, Idaho, USA. *Chemical Geology, 258*(3–4), 157–167.

Guimaraes, J. R. D., Betancourt, O., Miranda, M. R., Barriga, R., Cueva, E., & Betancourt, S. (2011). Long-range effect of cyanide on mercury methylation in a gold mining area in southern Ecuador. *Science of the Total Environment, 409* (23), 5026–5033.

Hiller, E., Lalinská, B., Chovan, M., Jurkovič, Ľ., Klimko, T., Jankulár, M., et al. (2012). Arsenic and antimony contamination of waters, stream sediments and soils in the vicinity of abandoned antimony mines in the Western Carpathians, Slovakia. *Applied Geochemistry, 27*(3), 598–614.

Hyun, S., Burns, P. E., Murarka, I., & Lee, L. S. (2006). Selenium(IV) and (VI) sorption by soils surrounding fly ash management facilities. *Vadose Zone Journal, 5*(4), 1110–1118.

Kerin, E. J., Gilmour, C. C., Roden, E., Suzuki, M. T., Coates, J. D., & Mason, R. P. (2006). Mercury methylation by dissimilatory iron-reducing bacteria. *Applied and Environmental Microbiology, 72*(12), 7919–7921.

Kyle, J. H., Breuer, P. L., Bunney, K. G., Pleysier, R., & May, P. M. (2011). Review of trace toxic elements (Pb, Cd, Hg, As, Sb, Bi, Se, Te) and their deportment in gold processing. Part 1: Mineralogy, aqueous chemistry and toxicity. *Hydrometallurgy, 107*(3–4), 91–100.

Lambertsson, L., & Nilsson, M. (2006). Organic material: the primary control on mercury methylation and ambient

methyl mercury concentrations in estuarine sediments. *Environmental Science and Technology, 40*(6), 1822–1829.

Lovitz, S.B. (2006). *Scales of responsible gold mining: overcoming barriers to cleaner artisanal mining in southern Ecuador. M.S. Thesis*. Burlington: The University of Vermont.

Machesky, M. L. (1990). Influence of temperature on ion adsorption by hydrous metal oxides. In R. L. Bassett & D. C. Melchoir (Eds.), *Chemical modeling of aqueous systems II* (American Chemical Symposium Series, Vol. 416). Washington: American Chemical Society.

Mitchell, C. P. J., Branfireun, B. A., & Kolka, R. K. (2008). Spatial characteristics of net methylmercury production hot spots in peatlands. *Environmental Science and Technology, 42*(4), 1010–1016.

Parkhurst, D. L., & Appelo, C. A. J. (1999). User's guide to PHREEQC (Version 2)—a computer program for speciation, batch-reaction, one-dimensional transport, and inverse geochemical calculations. US Geological Survey, Water-Resources Investigation Report 99–4259.

Ramirez-Raquelme, M. E., Ramos, J. F. F., Angelica, R. S., & Brabo, E. S. (2003). Assessment of Hg-contamination in soils and stream sediments in the mineral district of Nambija, Ecuadorian Amazon (example of an impacted area affected by artisanal gold mining). *Applied Geochemistry, 18*(3), 371–381.

Tarras-Wahlberg, N. H. (2002). Environmental management of small-scale and artisanal mining: the Portovelo-Zaruma goldmining area, southern Ecuador. *Journal of Environmental Management, 65*(2), 165–179.

Tarras-Wahlberg, N. H., & Lane, S. N. (2003). Suspended sediment yield and metal contamination in a river catchment affected by El Nino events and gold mining activities: the Puyango river basin, southern Ecuador. *Hydrological Processes, 17*(15), 3101–3123.

Tarras-Wahlberg, N. H., Flachier, A., Fredriksson, G., Lane, S., Lundberg, N., & Sangfors, O. (2000). Environmental impact of small-scale and artisanal gold mining in southern Ecuador—implications for the setting of environmental standards and for the management of small-scale mining operations. *Ambio, 29*(8), 484–491.

Tarras-Wahlberg, N. H., Flachier, A., Lane, S. N., & Sangfors, O. (2001). Environmental impacts and metal exposure of aquatic ecosystems in rivers contaminated by small scale gold mining: the Puyango River basin, southern Ecuador. *Science of the Total Environment, 278*(1–3), 239–261.

Taylor, H., Appleton, J. D., Lister, R., Smith, B., Chitamweba, D., Mkumbo, O., et al. (2005). Environmental assessment of mercury contamination from the Rwamagasa artisanal gold mining centre, Geita District, Tanzania. *Science of the Total Environment, 343*(1–3), 111–133.

USEPA Method 1630: Methylmercury in water by distillation, aqueous ethylation, purge and trap, and CVAFS, January 2001.

USEPA Method 1631, Revision E: mercury in water by oxidation, purge and trap, and cold vapor atomic fluorescence spectrometry, August 2002.

USEPA Method 1669: Sampling ambient water for trace metals at EPA water quality criteria levels, July 1996.

Velasquez-Lopez, P. C., Veiga, M. M., & Hall, K. (2010). Mercury balance in amalgamation in artisanal and small-scale gold mining: identifying strategies for reducing environmental pollution in Portovelo-Zaruma, Ecuador. *Journal of Cleaner Production, 18*(3), 226–232.

Velasquez-Lopez, P. C., Veiga, M. M., Klein, B., Shandro, J. A., & Hall, K. (2011). Cyanidation of mercury-rich tailings in artisanal and small-scale gold mining: identifying strategies to manage environmental risks in Southern Ecuador. *Journal of Cleaner Production, 19*(9–10), 1125–1133.

Williams, T. M., Dunkley, P. N., Cruz, E., Acitimbay, V., Gaibor, A., Lopez, E., et al. (2000). Regional geochemical reconnaissance of the Cordillera Occidental of Ecuador: economic and environmental applications. *Applied Geochemistry, 15*(4), 531–550.